



WASH 97- 206842

061347

DEPARTMENT OF ELECTRICAL & COMPUTER ENGINEERING
COLLEGE OF ENGINEERING AND TECHNOLOGY
OLD DOMINION UNIVERSITY
NORFOLK, VIRGINIA 23529

**DEVELOPMENT OF Ti:Al₂O₃ LASER FOR REMOTE SENSING
OF THE ATMOSPHERE**

By

Principal Investigator:
Dr. Hani Elsayed-Ali

Final Report

For the period December 31, 1997

Prepared for

National Aeronautics and Space Administration
Langley Research Center
Attn.: Joseph Murray, Officer
Mail Stop 126
Hampton, VA 23681-0001

Under

NASA GRANT NAG1-1578

Dr. Russell DeYoung, Technical Monitor
Mails Stop 401A
Hampton, VA 23681-0001

ODURF #141301

February 1997

DEPARTMENT OF ELECTRICAL & COMPUTER ENGINEERING
COLLEGE OF ENGINEERING AND TECHNOLOGY
OLD DOMINION UNIVERSITY
NORFOLK, VIRGINIA 23529

**DEVELOPMENT OF Ti:A12O₃ LASER FOR REMOTE SENSING
OF THE ATMOSPHERE**

By
Principal Investigator:
Dr. Hani Elsayed-Ali

Final Report
For the period December 31, 1997

Prepared for
National Aeronautics and Space Administration
Langley Research Center
Attn.: Joseph Murray, Officer
Mail Stop 126
Hampton, VA 23681-0001

Under
NASA GRANT NAG1-1
Dr. Russell DeYoung, Technical Monitor
Mails Stop 401A
Hampton, VA 23681-0001

ODURF #141301

February 1997



**Progress Report
of the Development of
Ti:Sapphire Laser System
for Lidar Measurement.**

1. Constructed second and third harmonic generation for the 867 nm leg, the harmonic generation wavelength is 433 nm and 289 nm respectively. Further optimization of the conversion efficiency is needed to be done.

Figure 1. Second Harmonic Generation (SHG) vs. Fundamental laser input energy. For 60 mJ 867 nm input laser energy, the output of the SHG is 1 mJ.

Figure 2. Time characteristics of the Third Harmonic Generation (THG at 289 nm). The FWHM of the THG is 26 ns, about 25% of the fundamental laser pulse.

2. Characterization of the new laser cavity and new power supply system.

Figure 3. Comparison of the flashlamp relative intensity vs. input energy at the Ti:Sapphire laser rod absorption region, with and without KFT-2 glass filter. Result indicates that about 3 time more intense at this region with the KFT-2 glass filter tube.

Figure 4. Comparison of the spectrum of flashlamp with and without KFT-2 filter

glass. On the left, without KFT-2, due to the cut-off frequency in the optical fiber, part of the spectrum at the UV region is not shown. There is a slightly decrease in the UV region and slightly increase in visible region with the KFT-2 filter. Not calibrated with standard source.

Figure 5. Flashlamp current vs. input energy. The FWHMs range from 5 to 7 microseconds.

Figure 6. Ti:Sapphire rod florescence vs. input energy. The FWHMs range from 8 to 14 microseconds.

3. Gain measurement of the new laser rod.

The new laser rod is with .1% w.t. Ti ions and with figure of merit (FOM) of 431.

Figure 7. Ti:Sapphire laser gain vs. input energy. The maximum gain at 198 J input energy is 1100%, indicating the high quality of the laser rod.

4. Construction of the new laser cavity.

With a new and better-quality laser rod, the construction of both the laser legs is completed. with the fundamental laser wavelength at 867 nm and 897 nm, respectively.

Figure 8. The Q-switched output from the fundamental laser wavelength of 867 nm and 897 nm respectively.

Figure 9. The output laser spectra for the 867 nm and 897 nm legs.

The 867 nm and 897 nm legs have been setup so that the laser system can laser alternatively at 867 nm and 897 nm with 2 Hz repetition rate.

5. Modeling of the Ti:Sapphire laser system.

Based on the output from the flashlamp fluorescence, the temperature profile of the plasma vs. time is modeled. Then the power emitted by flashlamp and absorbed by the Ti:Sapphire rod is calculated. The pumping of the laser rod is calculated. By solving the rate equations numerically, the temporal profile of laser level population inversion and photon density inside the cavity is obtained.

Figure 10. Laser population inversion and photon density vs. time at 50 J input.

Figure 11. Laser population inversion and photon density vs. time at 100 J input.

Figure 12. Laser population inversion and photon density vs. time at 200 J input.

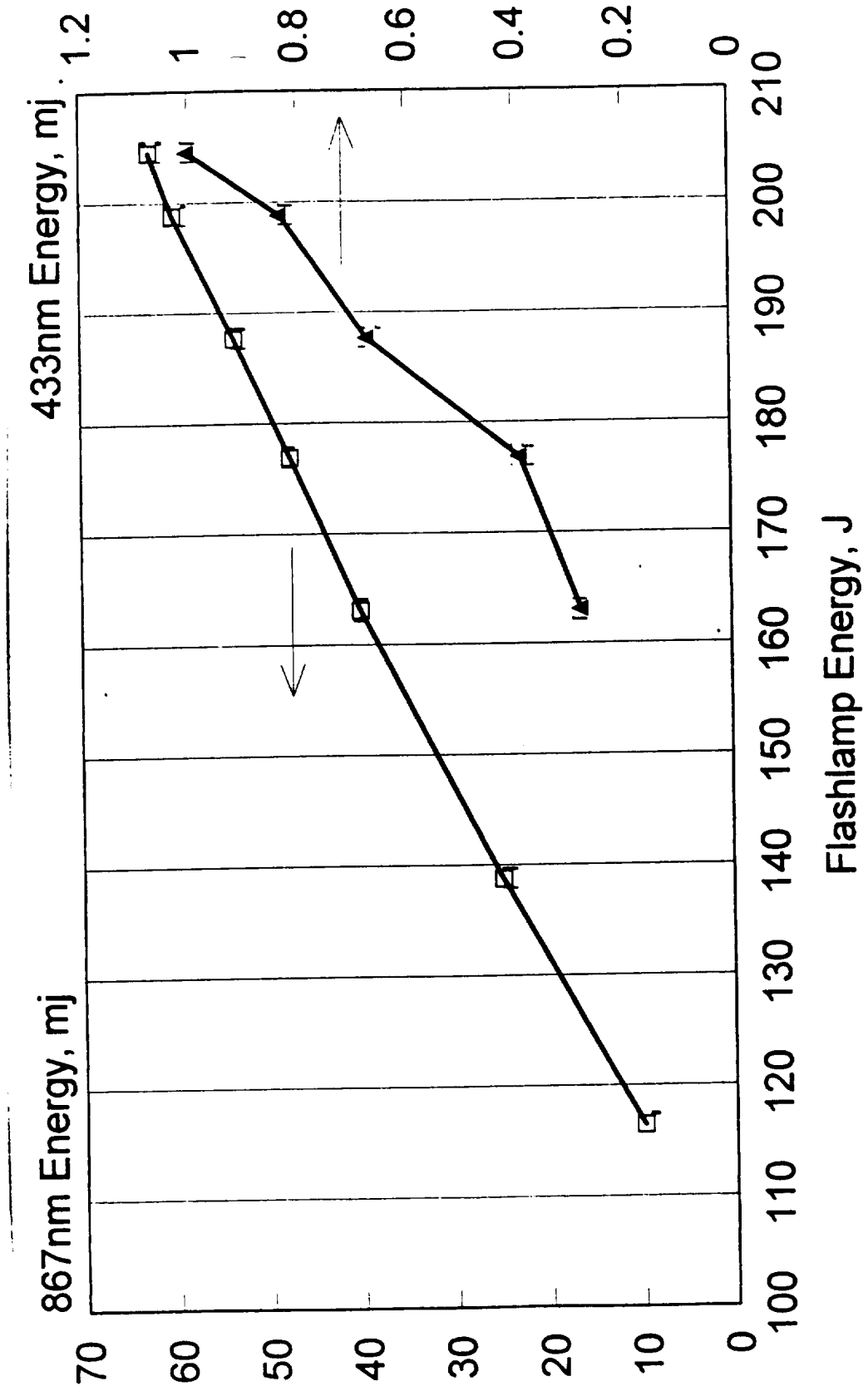


Figure 1. Second Harmonic Generation (SHG) vs. Fundamental laser input energy.

For 60 mJ 867 nm input laser energy, the output of the SHG is 1 mJ.

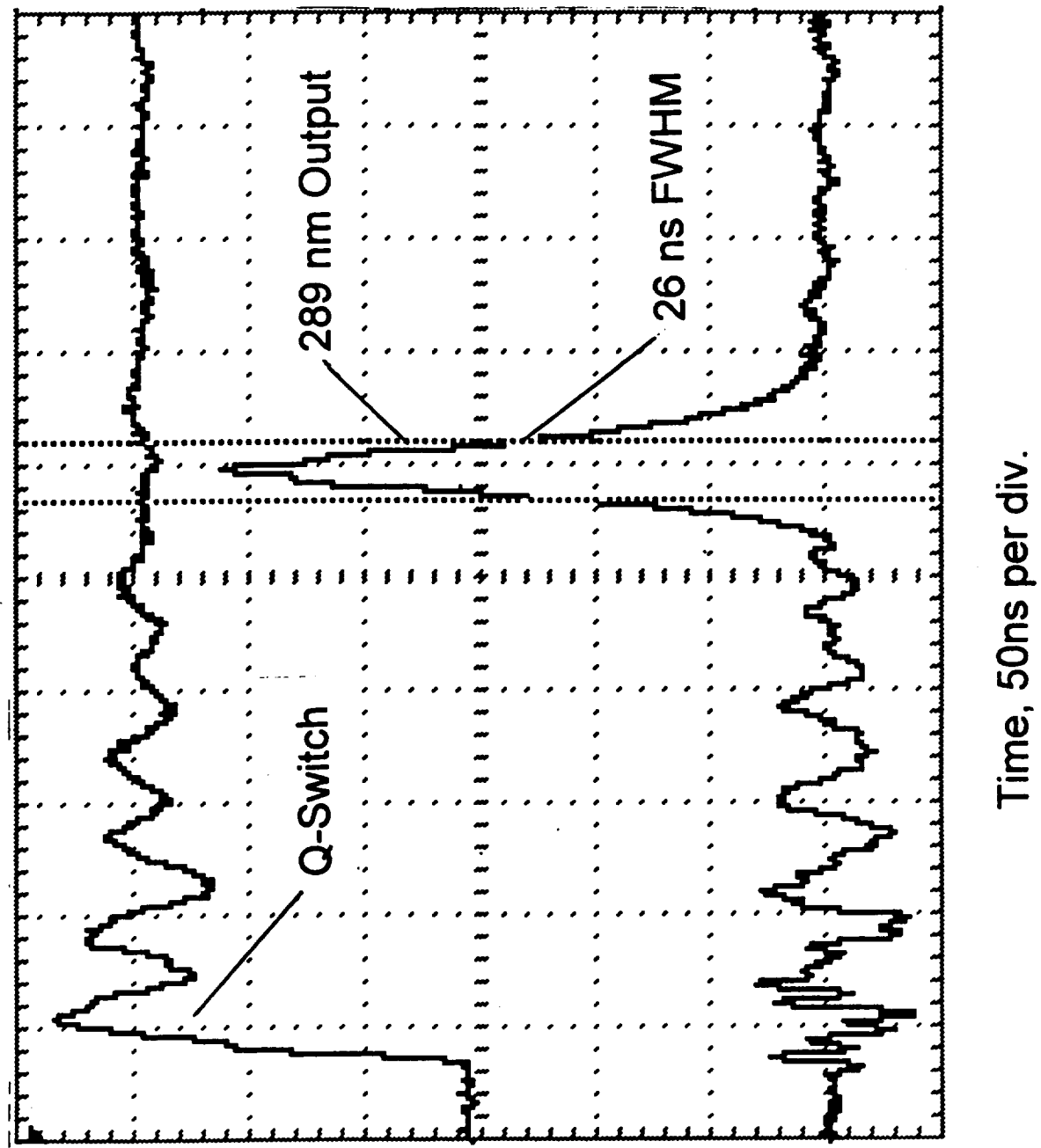


Figure 2. Time characteristics of the Third Harmonic Generation (THG at 289 nm). The FWHM of the THG is 26 ns, about 25% of the fundamental laser pulse.

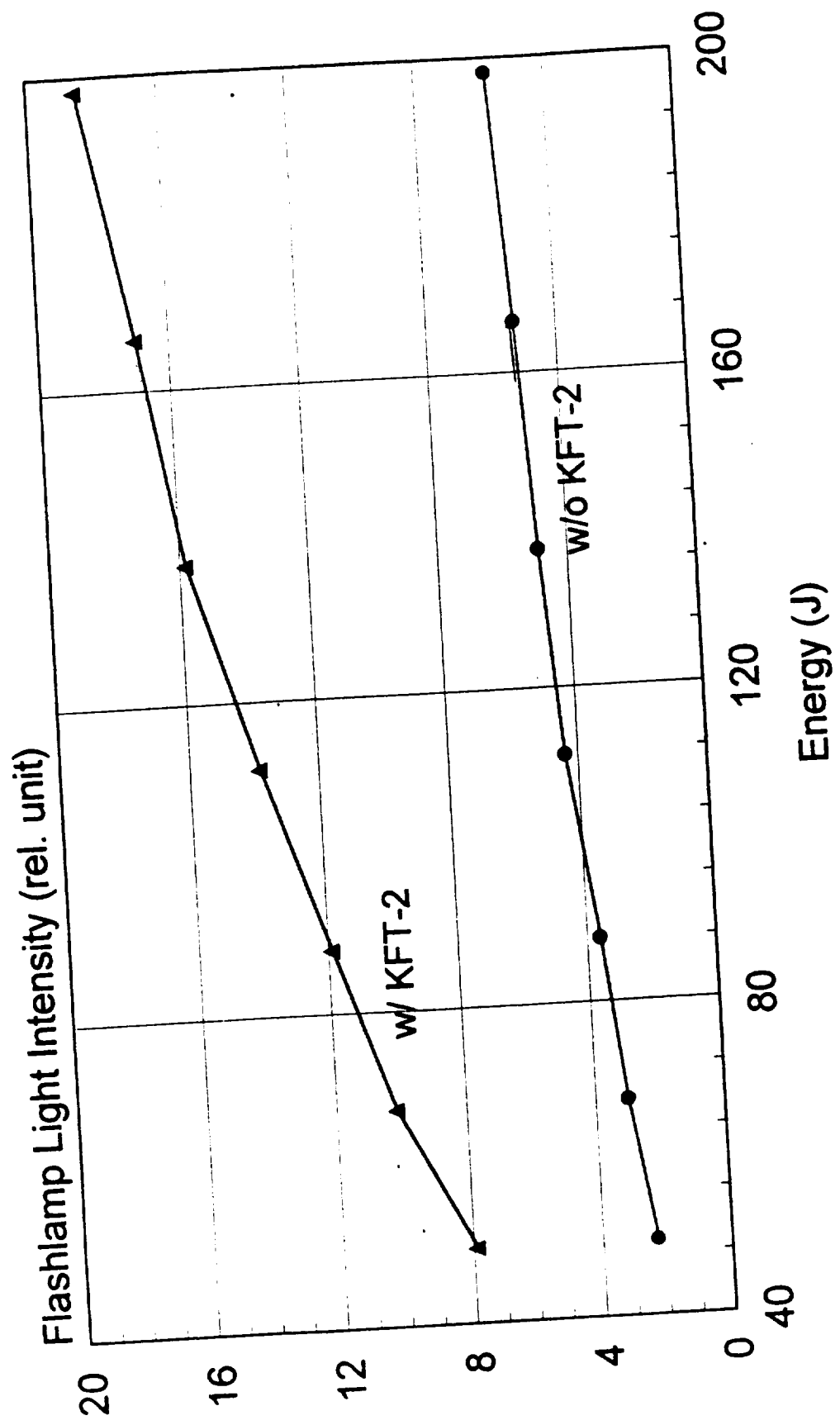


Figure 3. Comparison of the flashlamp relative intensity vs. input energy at the Ti:Sapphire laser rod absorption region, with and without KFT-2 glass filter. Result indicates that about 3 time more intense at this region with the KFT-2 glass filter tube.

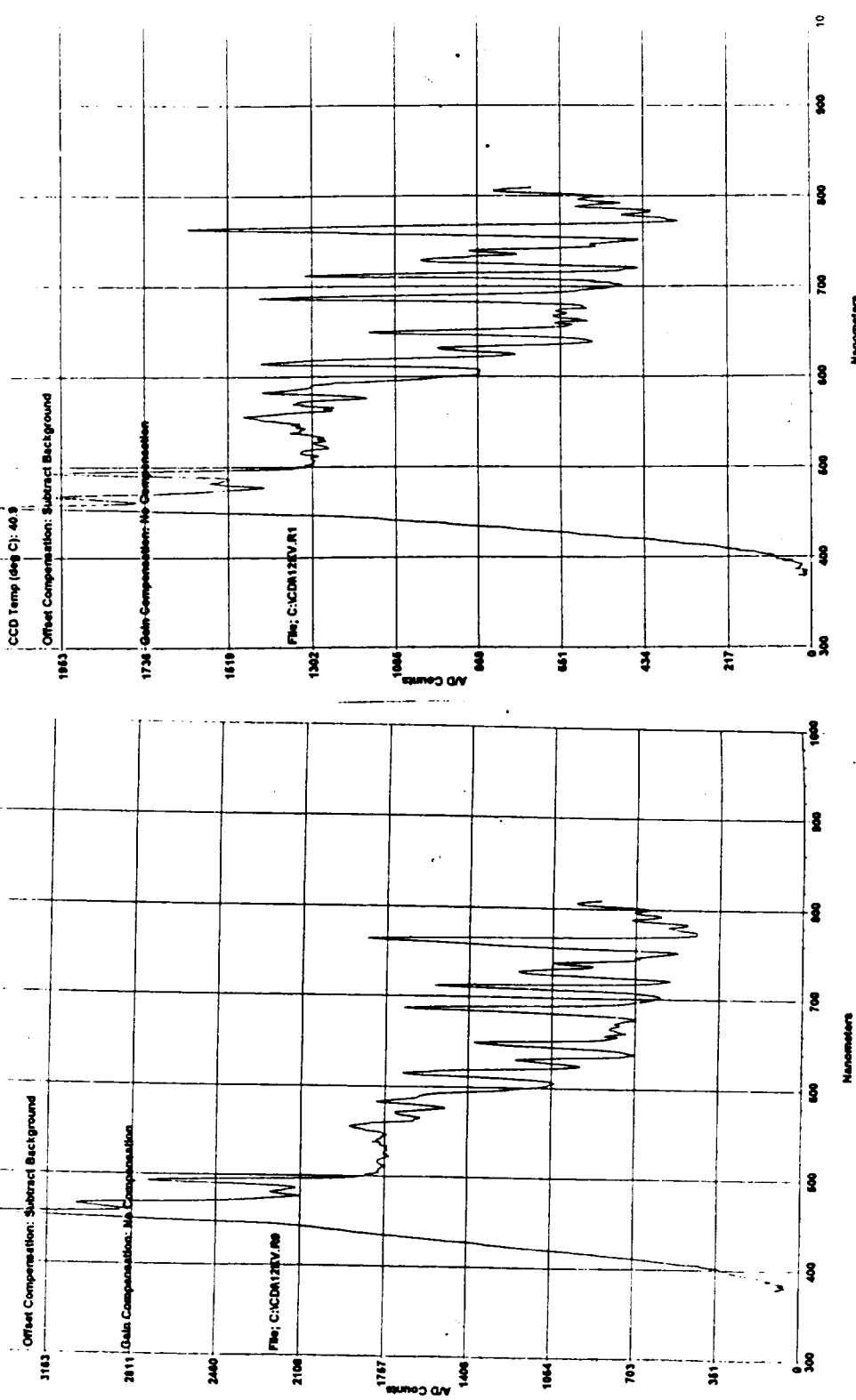


Figure 4. Comparison of the spectrum of flashlamp with and without KFT-2 filter glass. On the left, without KFT-2, due to the cut-off frequency in the optical fiber, part of the spectrum at the UV region is not shown. There is a slightly decrease in the UV region and slightly increase in visible region with the KFT-2 filter. Not calibrated with standard source.

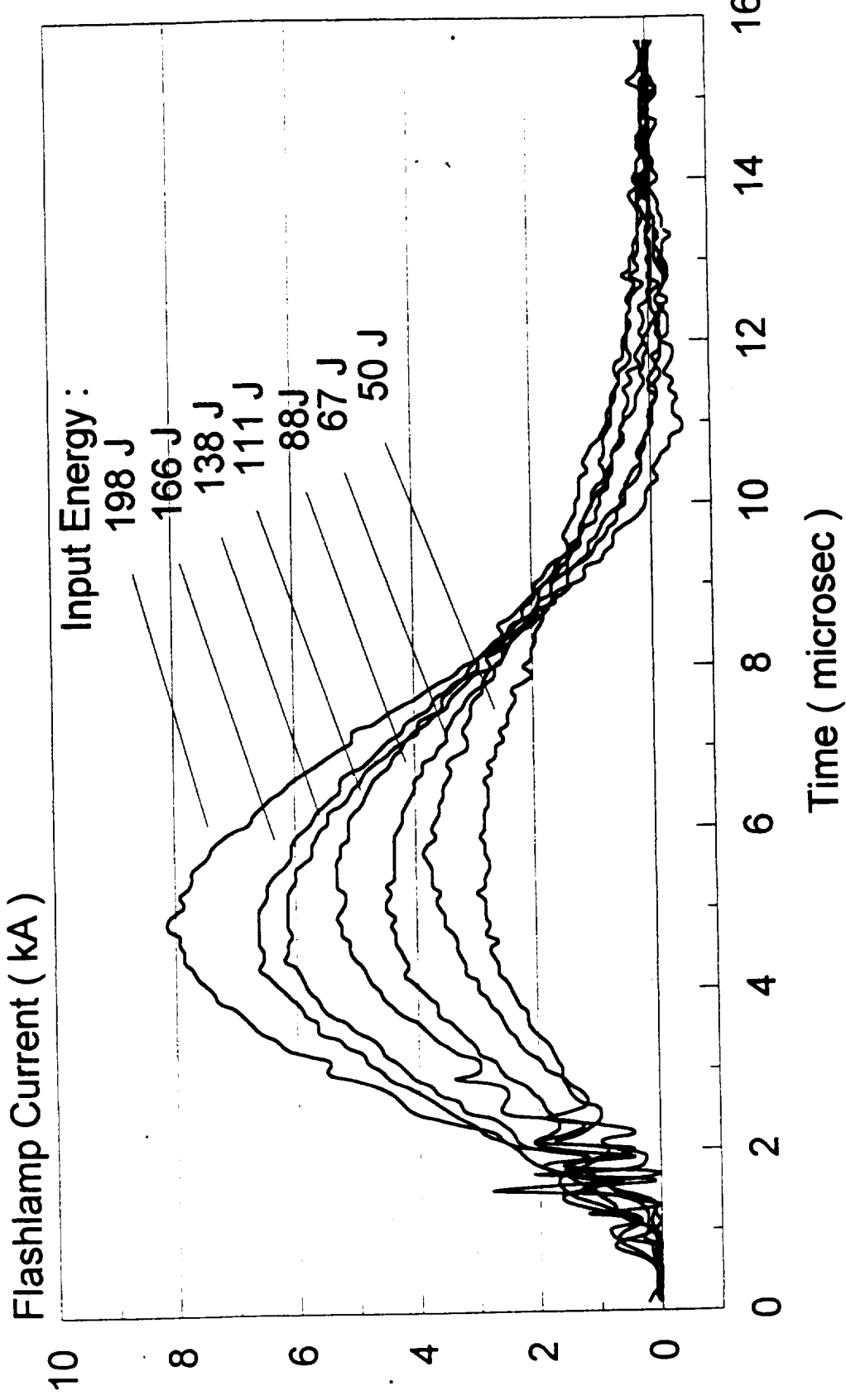


Figure 5. Flashlamp current vs. input energy. The FWHMs range from 5 to 7 microseconds.

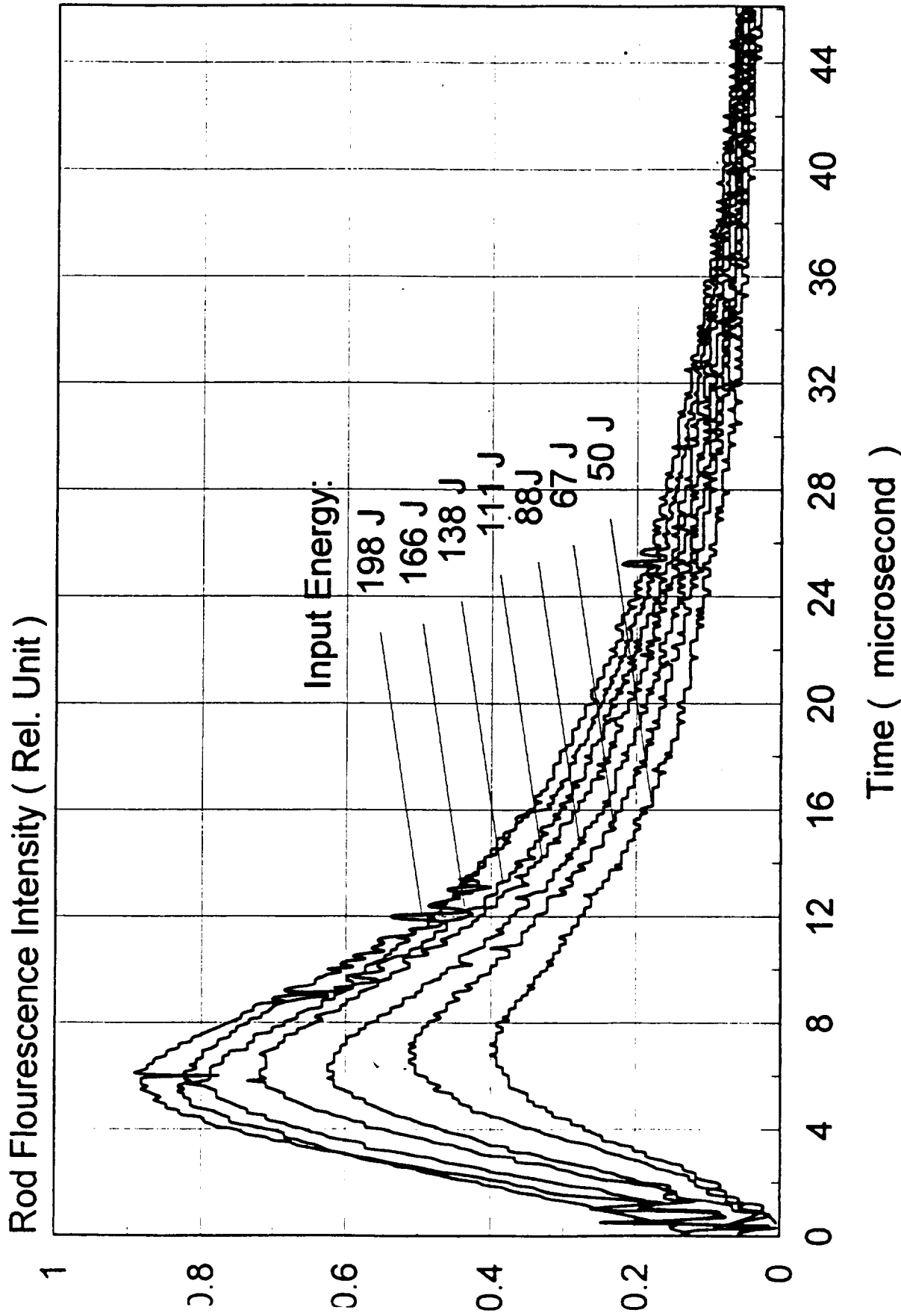


Figure 6. Ti:Sapphire rod fluorescence vs. input energy. The FWHMs range from 8 to 14 microseconds.

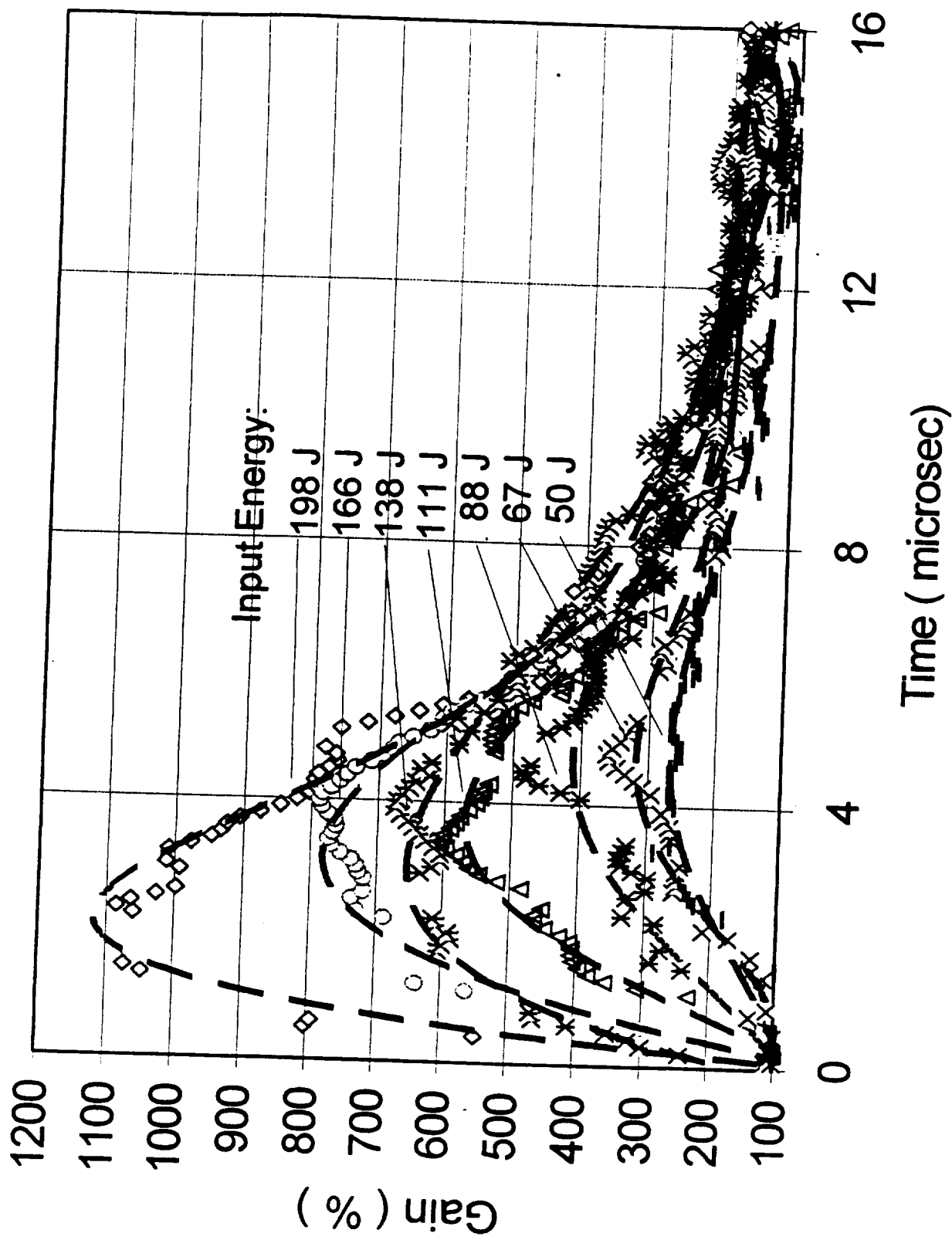


Figure 7. Ti:Sapphire laser gain vs. input energy. The maximum gain at 198 J input energy is 1100%, indicating the high quality of the laser rod.

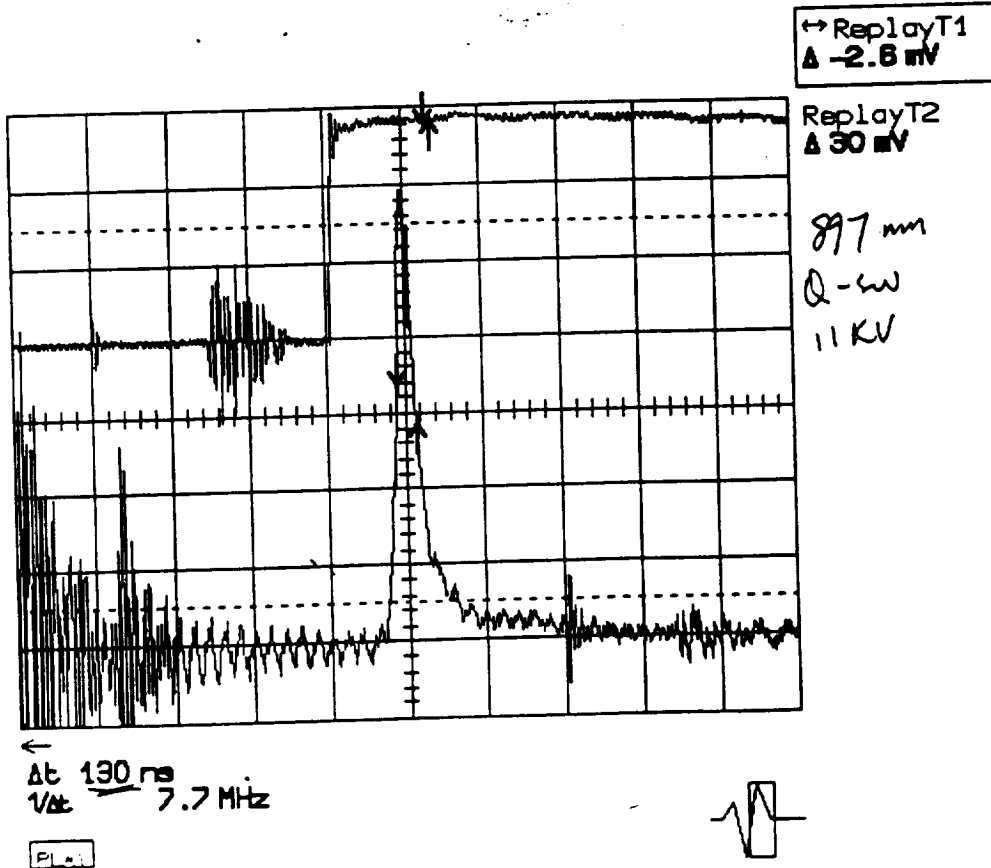
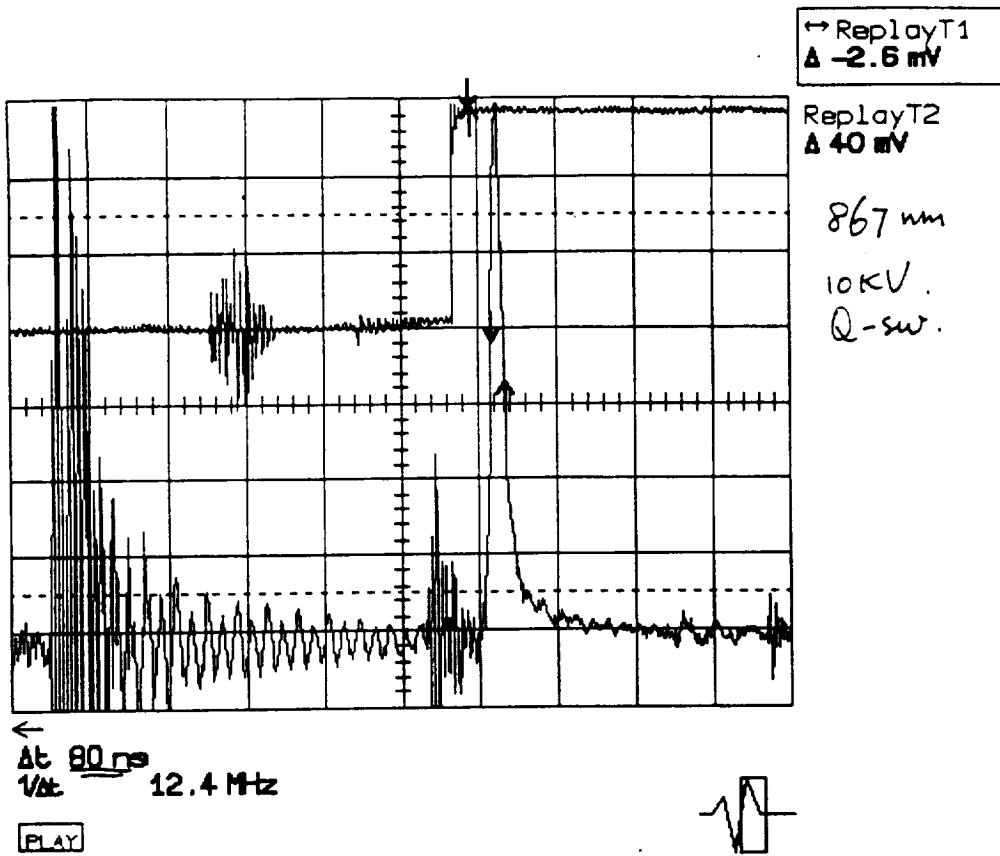


Figure 8. The Q-switched output from the fundamental laser wavelength of 867 nm and 897 nm respectively.

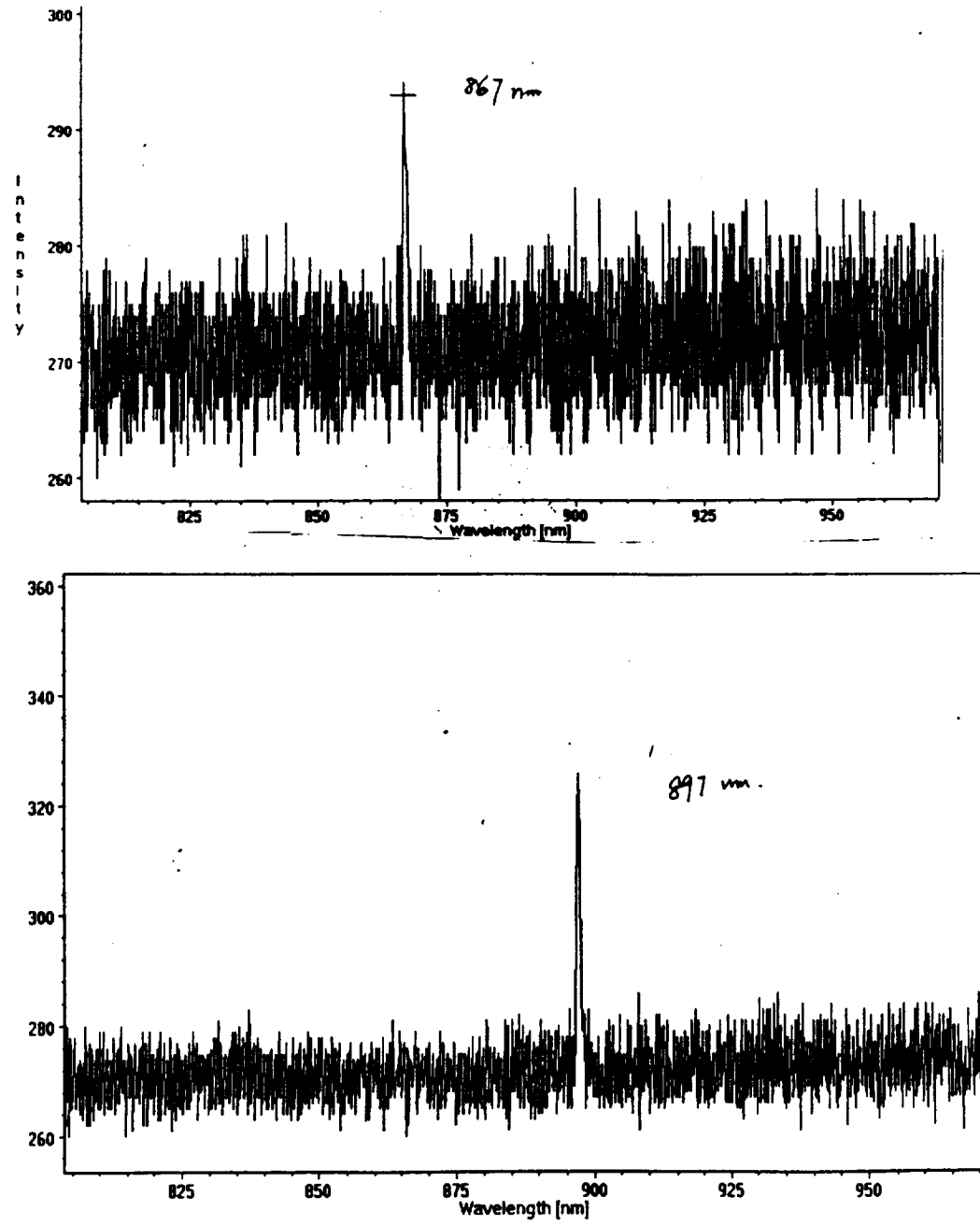


Figure 9. The output laser spectra for the 867 nm and 897 nm legs.

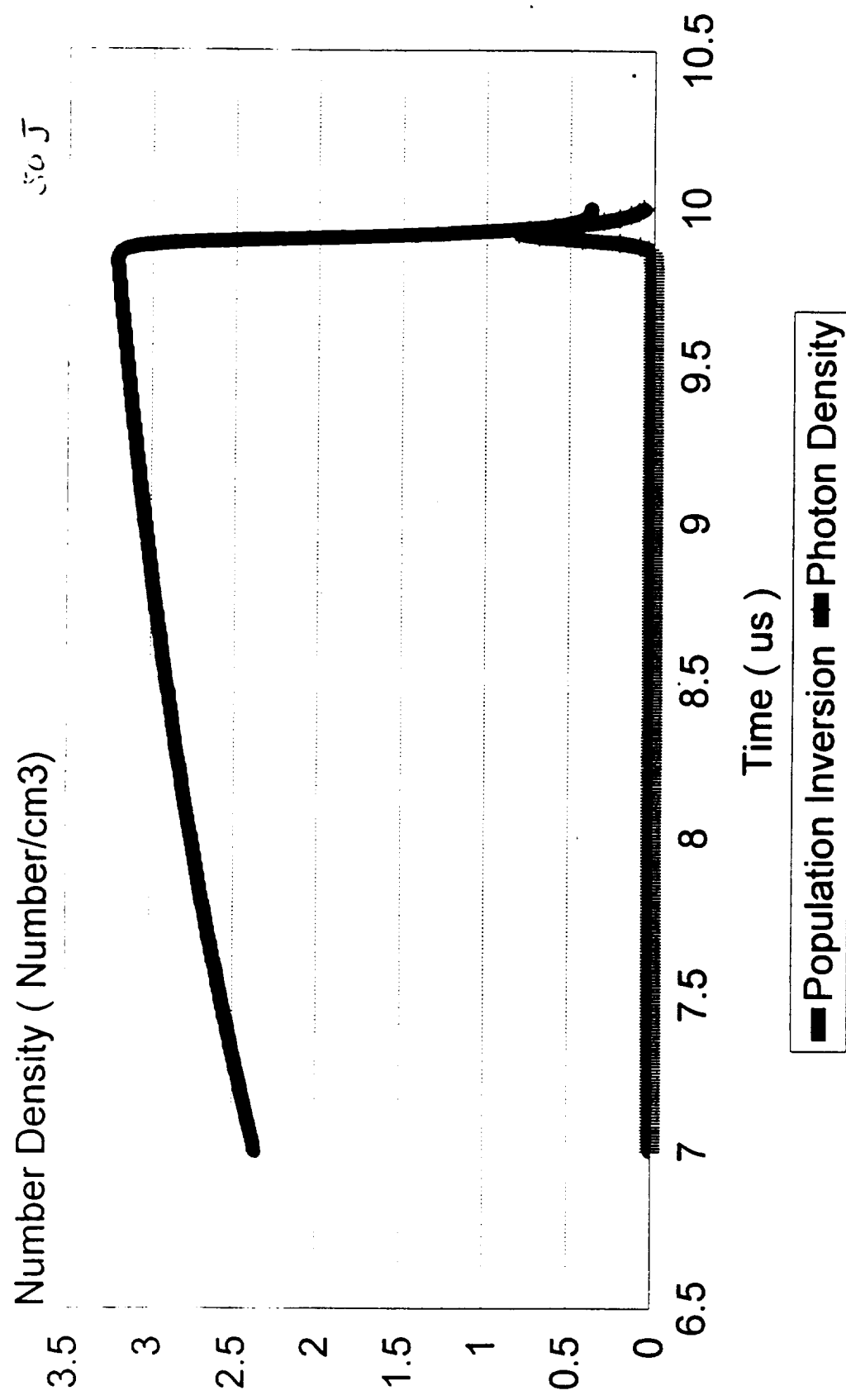


Figure 10. Laser population inversion and photon density vs. time at 50 J input.

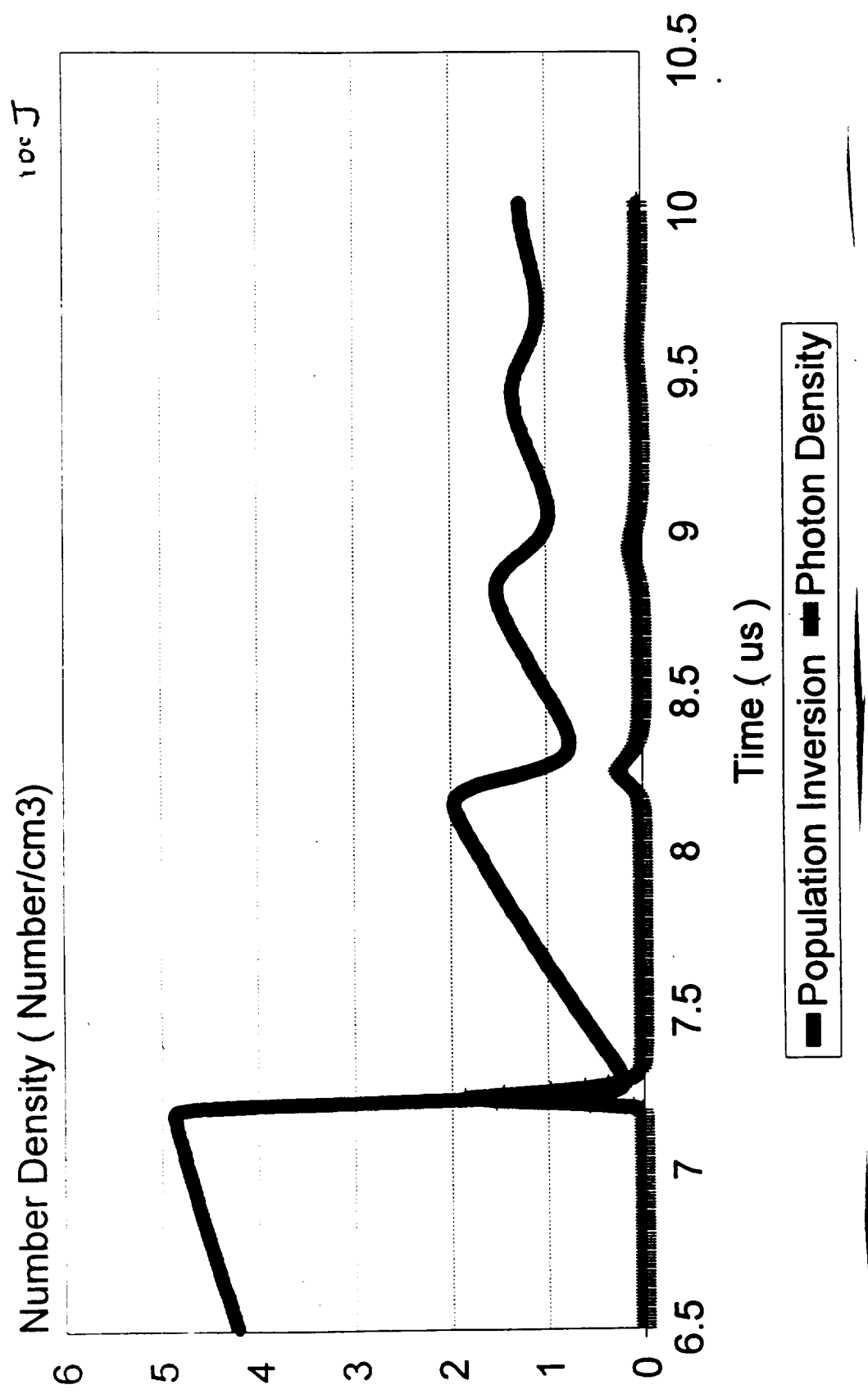


Figure 11. Laser population inversion and photon density vs. time at 100 J input.

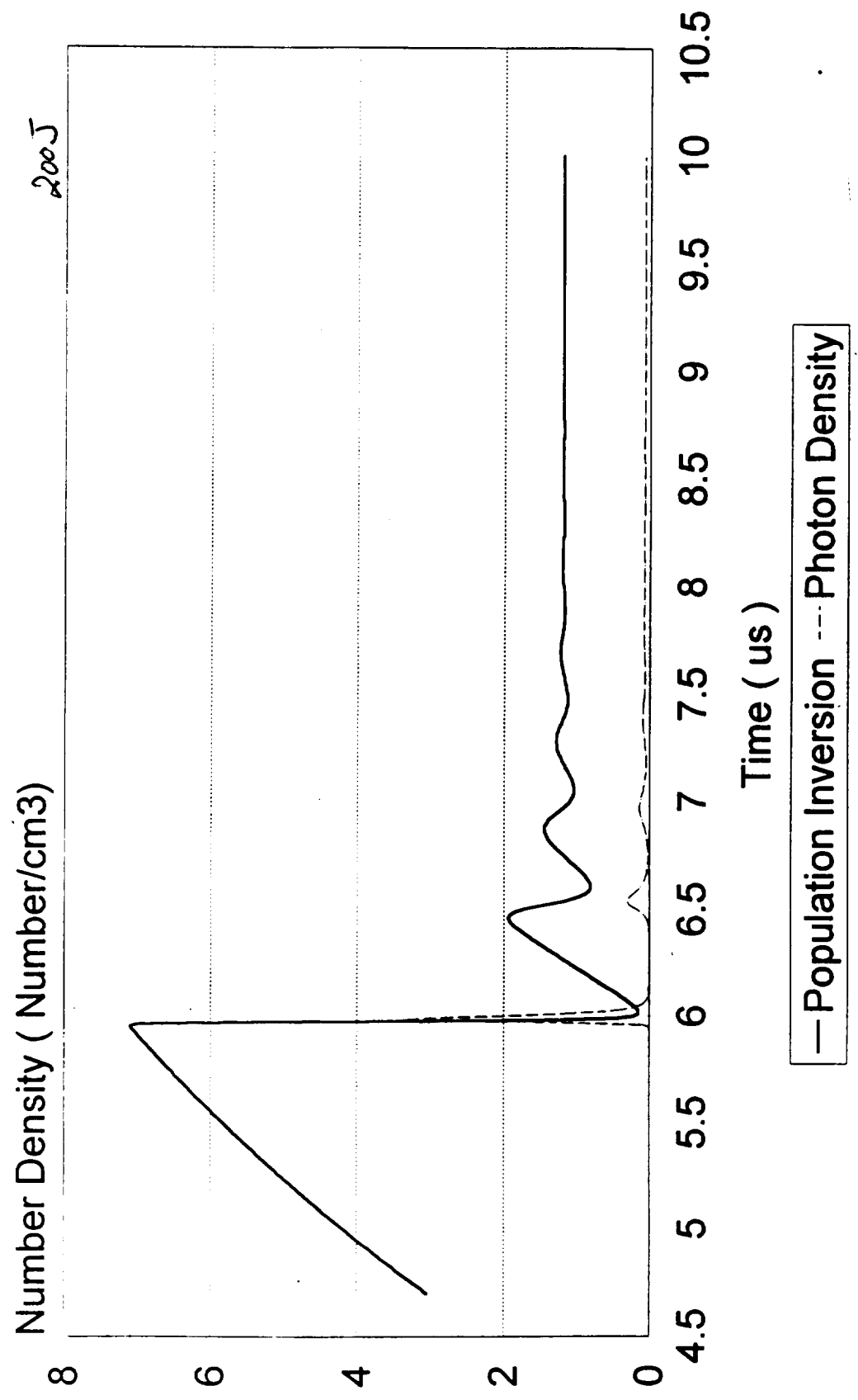


Figure 12. Laser population inversion and photon density vs. time at 200 J input.